Compliance of Thin Filaments in Skinned Fibers of Rabbit Skeletal Muscle

Hideo Higuchi,* Toshio Yanagida,*‡ and Yale E. Goldman§

*Yanagida Biomotron Project, 2-4-14 Senba Higashi, Mino, Osaka, Japan 562; ‡Department of Biophysical Engineering, Faculty of Engineering Science, Osaka University, Toyonaka, Osaka 560, Japan; and §Department of Physiology and Pennsylvania Muscle Institute, University of Pennsylvania, Philadelphia, PA 19104-6083 USA

ABSTRACT The mechanical compliance (reciprocal of stiffness) of thin filaments was estimated from the relative compliance of single, skinned muscle fibers in rigor at sarcomere lengths between 1.8 and 2.4 μm. The compliance of the fibers was calculated as the ratio of sarcomere length change to tension change during imposition of repetitive cycles of small stretches and releases. Fiber compliance decreased as the sarcomere length was decreased below 2.4 μm. The compliance of the thin filaments could be estimated from this decrement because in this range of lengths overlap between the thick and thin filaments is complete and all of the myosin heads bind to the thin filament in rigor. Thus, the compliance of the overlap region of the sarcomere is constant as length is changed and the decrease in fiber compliance is due to decrease of the nonoverlap length of the thin filaments (the I band). The compliance value obtained for the thin filaments implies that at 2.4-μm sarcomere length, the thin filaments contribute ~55% of the total sarcomere compliance. Considering that the sarcomeres are ~1.25-fold more compliant in active isometric contractions than in rigor, the thin filaments contribute ~44% to sarcomere compliance during isometric contraction.

INTRODUCTION

The sliding filament structure of the sarcomere in striated muscle (A. F. Huxley and Niedergerke, 1954; H. E. Huxley and Hanson, 1954) and the cross-bridge theory of muscle contraction (Hanson and H. E. Huxley, 1955; A. F. Huxley, 1957) imply that force actively generated by actomyosin is transmitted along the sarcomeres through the backbones of the thick (myosin containing) and thin (actin containing) filaments. Thus, the mechanical properties of the filaments are crucial parameters in hypotheses for the mechanism of contraction. Huxley and Simmons (1971) measured tension responses to quick length changes applied in actively force generating muscle fibers and found that the compliance of the fiber ($\Delta_{length}/\Delta_{tension}$ = strain/stress) corresponds to a decrease of length by 6 nm per half-sarcomere when tension is decreased from the active isometric value to zero. Improvements in technique reduced the 6-nm value to ~4 nm per half-sarcomere (Ford et al., 1977). A. F. Huxley and colleagues proposed that the thin and thick filament backbones are rigid. In that case, the filament lengths are constant and virtually all of the 4-nm length change is transmitted to the cross-bridges between the two sets of filaments.

Considering the filaments as rigid elements greatly simplified interpretation of mechanical experiments. Filament rigidity received support from several further mechanical studies on muscle fibers showing that fiber compliance scales with filament overlap (Ford et al., 1981; Tawada and Kimura, 1984) and changes only slightly over the plateau region of the length-tension curve (Julian and Morgan, 1981; Bagni et al., 1990). These studies suggested that the filaments are at least fivefold more stiff than the cross-bridges. The filaments would then contribute 20% or less of the total compliance in the sarcomere.

Fujime and co-workers pointed out, on the other hand, that flexural rigidity of actin filaments detected by dynamic light scattering (Fujime, 1970; Oosawa et al., 1973) implied an axial filament compliance that could explain the sarcomere compliance. However, the quantitative relationship between flexural rigidity and axial compliance requires details of the filament structure that are not accurately known. Recently Kojima et al. (1994) directly measured the strain (~1.5 nm/μm filament length) due to an applied stress (~100 pN) in single actin filaments in vitro. They estimated the contribution of actin filament compliance to be ~50% of the sarcomere compliance. Wakabayashi et al. (1994) and H. E. Huxley et al. (1994) showed by high resolution x-ray diffraction that the thin and thick filaments are extensible during contractions of living frog muscle. These recent results for the compliance of thin and thick filaments conflict with the proposal that the filaments are rigid and with earlier mechanical measurements on muscle fibers.

We investigated the compliance of thin filaments in skinned muscle fibers to determine accurately the contribution of thin filaments to sarcomere compliance. We measured the sarcomere compliance in the rigor condition (absence of ATP) at full overlap between the thick and thin filaments to avoid possible errors in experiments with actively contracting muscle due to variation in the proportion of myosin heads attached and to rapid tension recovery after

Received for publication 16 December 1994 and in final form 11 May 1995.

Address reprint requests to Dr. Yale E. Goldman, Department of Physiology, University of Pennsylvania School of Medicine, D700 Richards Building, 3700 Hamilton Walk, Philadelphia, PA 19104-6083. Tel.: 215-898-4017; Fax: 215-898-2653; E-mail: goldman@a1.mscf.upenn.edu.

0006-3495/95/09/1000/11 $2.00

applied length changes (Ford et al., 1981). Compliance at the ends of the fiber was avoided by accurately measuring sarcomere length changes using light diffraction. In the sarcomere length range from 2.4 to 1.8 μm, sarcomere compliance varies mainly due to alterations in the length of the nonoverlap region of the thin filaments (the I bands) and, thus, is sensitive to thin filament compliance. The present results suggest that thin filaments are extensible and contribute ~55% of the total sarcomere compliance in rigor and ~44% during active contraction. Some of the results have been reported briefly (Higuchi et al., 1994).

MATERIALS AND METHODS

Fiber preparation and mechanical measurements

Glycerol-extracted fibers from rabbit psoas muscle were prepared as described by Goldman et al. (1984). Fiber bundles were stored at −20°C in 50% glycerol for 5–14 days. Single fibers were dissected from the bundles in silicone oil (Dow Corning, silicone 200 fluid) at ~10°C. A fiber segment, ~3 mm long and ~80 μm in diameter, was attached horizontally, using T-shaped aluminum clips, to hooks on a strain-gauge tension transducer (AE801, Akers, Horten, Norway, resonant frequency 5 kHz) and a linear, moving-coil motor capable of applying length steps complete within 200 μs, kindly supplied by Dr. V. Lombardi (University of Florence, Florence, Italy).

Sarcomere length measurement and data recording

The sarcomere length of a central region of the fiber, ~2 mm in length, was measured by a white light diffraction method that avoids the Bragg-angle artifact present in laser diffraction experiments (Goldman, 1987). As set up here, the spatial resolution of the diffraction instrument was 0.25 nm per half-sarcomere for single-sweep recording at 36-μs time resolution. Tension and position of the motor were monitored continuously on a chart recorder. For compliance measurements, the tension, motor position, and sarcomere length signals were digitized at 5-kHz sampling rate by a digital storage oscilloscope (Nicolet, model Pro40). Data were stored on diskettes and analyzed on a 80486-based computer using software written in-house.

Experimental procedure

A single, skinned fiber was mounted in an experimental trough in relaxing solution (Table 1) at a sarcomere length of ~2.3 μm and then treated for 5–10 min with 0.5% Triton X-100 in relaxing solution to remove residual membrane components. All procedures were performed at 10 ± 1°C. Compositions of solutions are listed in Table 1. The fiber was transferred into rigor solution, and then the length, width, and height of the fiber were measured using a compound microscope with a graticule in the eyepiece. The cross-sectional area was calculated as $\pi/4 \times$ [extreme width] × [height at the center of the fiber] (Goldman and Simmons, 1984). The fiber was then placed in relaxing solution again.

A procedure was required to reduce the length of fibers below the slack length while keeping the cross-striations uniform. The fiber was first put into activating solution containing 50 mM 2,3-butanedione 2-monoxime (Act-BDM in Table 1) for ~0.5 min. In this solution, the fiber would actively shorten below slack length (Fig. 1), but isometric tension development was suppressed (<2% of the normal active tension, Higuchi and Takemori, 1989). The fiber was allowed to shorten to a sarcomere length of 1.7–2.1 μm and then put into rigor by immersion in Ca-Rigor-BDM solution. Finally, the fiber was transferred to a trough containing the rigor solution without Ca or BDM for compliance measurements. The beam of the white light diffraction instrument for measuring sarcomere length (Goldman, 1987) was adjusted onto the fiber, and the static sarcomere length was recorded. The fiber was slowly stretched using a micrometer screw on the transducer mount until the tension was ~150 kN/m^2 and then subjected to series of ~20 repeated 1–2 nm per half-sarcomere stretch/release pulses at each of 11 tension levels from the ~150 kN/m^2 value downward to zero (Fig. 1). The length pulses were generated by a pulse generator (Wavetek, model 116) and superimposed on a staircase of 0.3- to 0.6-nm releases, generated by a digital-to-analog convertor driven from a binary counter circuit, to obtain the 11 tension levels. The slow stretch and stepwise pulse sequence were repeated 2–4 times in each rigor contraction (Fig. 1). Sarcomere length was monitored by optical diffraction before and after each test length sequence to check for changes. The fiber was then immersed in relaxing solution again and set to a new sarcomere length for the next rigor contraction.

Equation for estimating the compliance of thin filaments

We estimated the thin filament compliance from the variation of fiber compliance with sarcomere length by a modification of the method used by Bagni et al. (1990). We assumed that 1) compliance of the overlap region between thin and thick filaments stays constant at sarcomere length (L) shorter than full overlap length (L_o), 2) compliance of the Z line and bare zone of the thick filament are independent of sarcomere length, 3) compliance of the thin filament is uniform along its length, and 4) parallel compliances in the sarcolemma and connectitin (connectin, titin) are large enough to be ignored at $L < L_o$. The bases for these assumptions are given in Discussion. Under these conditions, compliance (c_s) of a half-sarcomere at $L < L_o$ is given by

$$c_S = L_I \cdot C_I + L_R \cdot C_R, \quad (1)$$

where L_I is the length in μm of thin filaments not interacting with myosin heads, i.e., L_I is half the length of the I band excluding the Z line. C_I is compliance per μm length of the thin filaments. $L_R \cdot C_R$ is the compliance in the remainder of the half-sarcomere, e.g., overlap region, thick filament bare zone, and Z line. $L_R \cdot C_R$ is assumed to be constant in the present experiments.

The structure of sarcomere in the experimental range of lengths is shown in Fig. 2. The length of the thin filament (from tips to the center of

TABLE 1 Composition of solutions

Solution	Na_2ATP	$MgCl_2$	EGTA	Ca-EGTA	HDTA	BDM
Relaxing	1.1	4.1	51	0	0	0
Rigor	0	3.2	53	0	0	0
Act-BDM	1.1	1.3	0	20	33	50
Ca-Rigor	0	1.3	0	20	33	0
Ca-Rigor-BDM	0	1.3	0	20	33	50

Concentrations in mM. All solutions contained 10 mM reduced glutathione and 100 mM *N*-tris(hydroxymethyl)methyl-2-aminoethanesulphonic acid (TES) buffer. Ca-EGTA, equimolar total Ca and EGTA; HDTA, 1,6-diaminohexane-*N,N,N′,N′*-tetraacetic acid; BDM, 2,3-butanedione 2-monoxime.

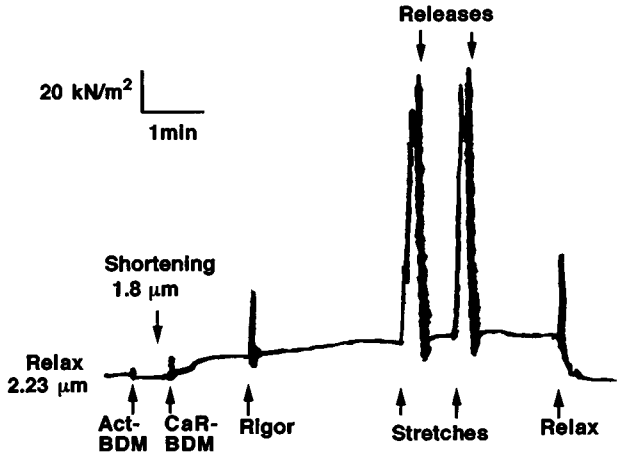

FIGURE 1 Chart recording of the tension from a fiber showing the protocol for measurement of compliance. The fiber was initially in relaxing solution at a sarcomere length of 2.23 μm. The fiber was then transferred into Act-BDM solution and was shortened to 1.80 μm. The fiber was put into Ca-Rigor-BDM solution (CaR-BDM) and then into rigor solution. After several minutes to allow complete exchange of the fiber interior, the fiber was stretched manually until the tension reached ~150 kN/m² and then subjected to 21 repeated stretch/release pulses superimposed on each step of a staircase of releases that successively reduced tension toward zero. The same manual stretch and stretch/release/staircase waveform was applied again. Finally, the fiber was placed in relaxing solution. Fiber dimensions: length 2.98 mm, cross-sectional area 6010 μm², T = 10°C.

the Z line) was taken to be 1.12 μm (Sosa et al., 1994). The bare zone of the thick filament was taken as 0.16 μm (Craig, 1977). L_o (maximum full overlap length) is (twice the thin filament length) + (bare zone of the thick filament) = 2 × 1.12 + 0.16 = 2.40 μm. L_I can be written as $(L - L_M - L_Z)/2$, where L_M is the length of the thick filaments (1.63 μm), (Sosa et al., 1994) and L_Z is the axial width of the Z line (0.067 μm, Schachat et al., 1985). $L_I = \frac{1}{2}L - 0.85$ μm. $L_R = (L_M + L_Z)/2 = 0.85$ μm. At $L < 2.40$ μm, Eq. 1 then becomes

$$c_S = (\tfrac{1}{2}L - 0.85) \cdot C_I + 0.85 \cdot C_R. \quad (2)$$

Because C_R is constant as sarcomere length changes, C_I can be estimated from the variation of c_S with L.

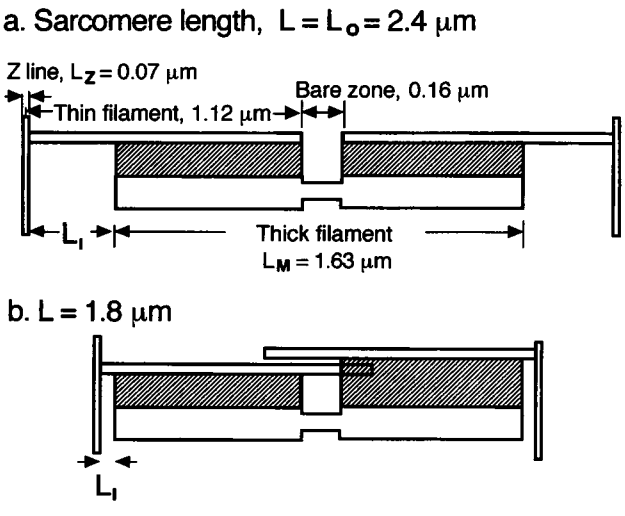

FIGURE 2 Schematic illustration of the structure of the sarcomere at lengths of 2.4 μm (*a*) and 1.80 μm (*b*). The maximum length with full overlap (L_o) is 2.4 μm; L_Z, width of Z line (0.07 μm); L_M, the length of thick filament (1.63 μm); L_I, half-length of the I band excluding the Z line (variable).

RESULTS

Compliance measurements

To determine the compliance of the thin filaments, we measured sarcomere length and tension changes during applied steps at sarcomere lengths shorter than 2.4 μm. In Ca-activating solution with 50 mM BDM, active tension was suppressed to <2% of its normal value (~150 kN/m²), but the fibers would still shorten actively below slack length (2.2 μm). Even when active tension was <1% of the normal value, fibers would shorten to 1.8-μm sarcomere length or less. This result indicates that the internal force resisting shortening below 2.2 μm due to double-overlap of the thin filaments is negligibly small. When ATP was taken away with BDM present (Ca-Rigor-BDM in Fig. 1), the fibers did produce tension. Once the fiber was in rigor, sarcomere length uniformity was estimated by directly measuring the spacing of 10 striations at three to five positions along the fiber under a compound microscope. The standard deviations of sarcomere lengths were 0.030 μm (n = 5) and 0.031 μm (n = 24) at sarcomere length of 2.2–2.4 and 1.7–2.0 μm, respectively. These data show that the protocol, using BDM to obtain shortened sarcomeres and to induce rigor, successfully maintained uniformity along the fibers.

After fibers were stretched manually to increase rigor tension to ~150 kN/m², which corresponds to active tension at 10°C (Figs. 1 and 3), a sequence of repeated stretch-release pulses superimposed on a staircase of small length releases was applied to measure compliance over a range of tensions. A staircase of 11 steps, each 0.3–0.6 nm per half-sarcomere (Figs. 1 and 3 *a*), decreased tension successively down from ~150 kN/m² to zero. At each tension level, the fiber was stretched repeatedly and released 0.5–2 nm per half-sarcomere. Fig. 3 shows tension and sarcomere length for the whole pulse sequence (*a*) and the 21 pulses at the highest tension (*b*). The top set of recordings (*a–d*) was made at 1.80 μm, corresponding to the record in Fig. 1, and the bottom ones (*e* and *f*) at 2.37 μm. At each tension level, the 21 stretch-release pulses were averaged together to improve the signal-to-noise ratio. Fig. 3, *c* and *e* show the average of the 21 tension and sarcomere length pulses at the highest tension. Fig. 3, *d* and *f* show averaged tension and sarcomere length pulses at tensions obtained during each of the first 10 steps of the staircase. These average records could be measured to 1% resolution providing accurate relative values of compliance. The static striation spacing, monitored by light diffraction, was not altered appreciably after the whole stretch-staircase sequence.

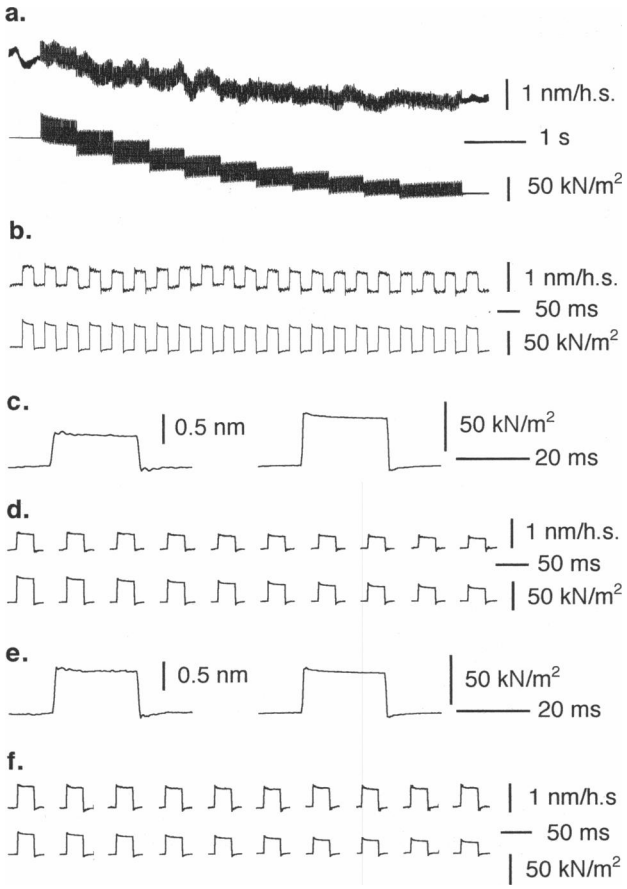

FIGURE 3 Tension and sarcomere length changes in response to imposed length changes in a skinned fiber in rigor. Upper (*a*, *b*, *d*, and *f*) or left (*c* and *e*) traces in each panel are the sarcomere length. The accompanying lower or right-hand traces are tension. The traces came from the experiment of Fig. 1. For *a–d*, the sarcomere length was 1.80 μm, the first pulse sequence shown in Fig. 1. For *e* and *f*, the sarcomere length was 2.37 μm. (*a*) The whole sequence of 21 repeated stretch/release pulses superimposed on each step of a staircase. (*b*) The first 21 stretch/release pulses at the highest tension in *a*. The striation spacing signal in *b* was filtered with a 120-Hz notch filter to remove mains ripple. The slow random deflections of the striation spacing traces in *a* and *b* are drift in the sarcomere length detector and do not affect the averaged deflections of striation spacing in *c–f*. (*c* and *e*) Sarcomere length and tension signals averaged over the 21 repeated pulses. (*d* and *f*) Averaged length and tension signals for first 10 steps of the staircases applied at 1.80 and 2.37 μm, respectively. The 11th step was not included in the analysis because the striation signal was not reliable if the muscle fiber went slack. h.s., half-sarcomere. Fiber dimensions and conditions are as in Fig. 1.

Fiber compliance was calculated from the ratio of averaged sarcomere length change to averaged tension change (Fig. 3 *c–f*). To avoid the small amount of stress relaxation seen in the tension traces, both tension and striation signals were measured during the final ~10 ms before each length change. Although the amplitude of the pulse length changes was kept constant, sometimes the sarcomere length changes varied during the staircase due to series compliances at the attachment points (Fig. 3 *d*). This end compliance did not affect measurement of fiber compliance because the striation spacing signal came from a central region of the fiber preparation.

The compliance was measured 2–4 times at each sarcomere length. Fig. 4 *a* shows compliance values for the fiber used for Figs. 1 and 3, plotted against the tension value at the middle of each averaged tension pulse. The compliance decreased as the tension increased, indicating nonlinearity of the sarcomere compliance. The change of compliance with sarcomere length was reproducible; for instance,

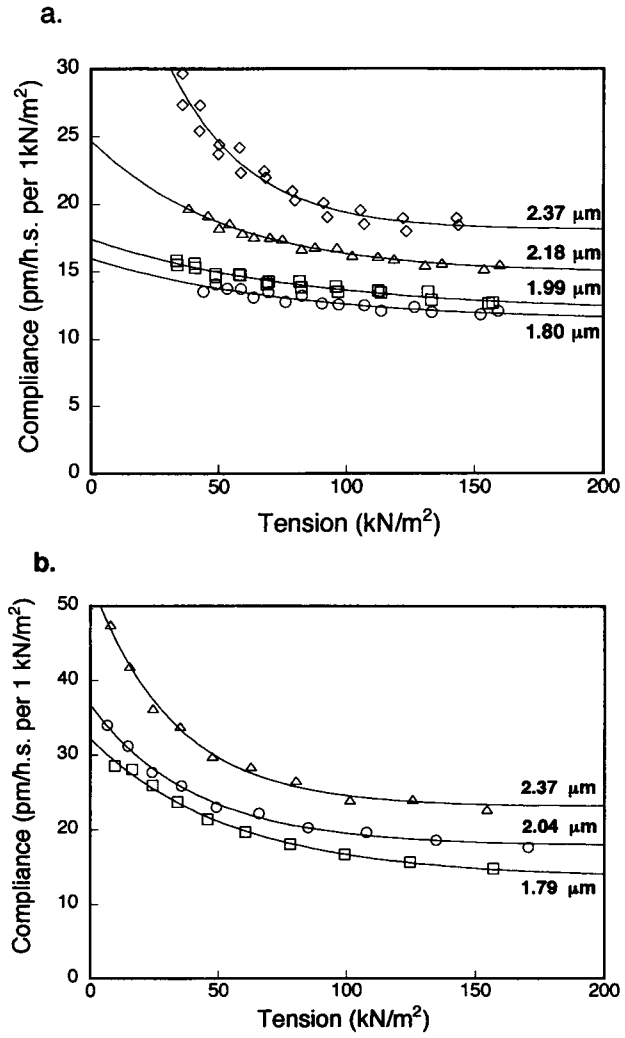

FIGURE 4 Compliance changes with tension and sarcomere length of a fiber. Compliance was calculated as the ratio of half-sarcomere length change to tension change using averaged sarcomere length pulses and averaged tension pulses such as those in Fig. 3 *c–f*. The abscissa is the tension value measured in the middle of each averaged tension pulse. Data were taken from recordings duplicated at each sarcomere length as in Fig. 1. Symbols in *a*: ◇, 2.37 μm; △, 2.18 μm; □, 1.99 μm; ○, 1.80 μm. Data in *a* are from the same experiment shown in Figs. 1 and 3. *b* came from a different fiber, symbols: △, 2.37 μm; ○, 2.04 μm; □, 1.79 μm. The compliance at each sarcomere length was fitted by the curve $c_s = a + b \cdot \exp(-T/c)$ (Eq. 3 in text), where c_s and T are measured compliance and tension, respectively, and a, b, and c are determined by least-squares. The units for the abscissa are pm stretch per half-sarcomere for each 1 kN/m² force increase.

the measurements in Fig. 4 *a* were made in the order 1.80, 2.18, 1.99 and, finally, 2.37 μm. Compliance values from test sequences repeated at a given sarcomere length and tension were very close to each other.

Depending on the fiber length, in some fibers the length step sequence did not bring tension down to the baseline as in Fig. 4 *a*. Fig. 4 *b* shows data from a different fiber that did yield data extending to the tension baseline. The form of the data was similar.

Estimation of thin filament compliance

Fiber compliance was interpolated to tension values of 50, 100, 150, and 200 kN/m^2 by fitting the following exponential relation to data from each sarcomere length as in Fig. 4:

$$c_S = a + b \cdot \exp(-T/c), \quad (3)$$

where c_S and T are measured sarcomere compliance and tension, respectively, and a, b, and c are parameters determined by least-squares fitting (Fig. 4). Compliance was fitted very well by Eq. 3 in the range of tensions tested, 10–170 kN/m^2; correlation coefficients averaged 0.99. Compliance at a given tension was calculated using Eq. 3 with the parameters fitted to the data, and the results from the fiber of Fig. 4 *a* are plotted for two tension levels in Fig. 5. Compliance decreased as the fibers were shortened. The data in Fig. 5 were then fitted with Eq. 2 to give values of C_I, the compliance of the thin filaments per μm length, and $L_R \cdot C_R$, the compliance of the remainder of the sarcomere. The solid lines in Fig. 5 show the fitted relation between sarcomere compliance and sarcomere length; C_I is given by the slope of the lines.

Because the data from the shortest lengths were obtained with double-overlap of the thin filaments (see Fig. 2 *b*), we also analyzed the data from each fiber at sarcomere lengths $\geq$2.0 μm. The dashed lines in Fig. 5 represent Eq. 2 fitted to the data at $\geq$2.0 μm in this fiber. In most experiments, the slopes of the lines and, thus, the estimated values of C_I, were unchanged or slightly higher when data were restricted to $\geq$2.0 μm.

The changes of sarcomere compliance (c_S), actin filament compliance (C_I), and remaining compliance (C_R) with tension at 2.4-μm sarcomere length are summarized for a series of fibers in Fig. 6. C_I corresponds to 15.6–23.0 pm (average 18.9 pm) stretch per μm of filament length per 1 kN/m^2 force increase in the 100–200 kN/m^2 force range. All three compliances decreased as tension increased. C_I and C_R have similar magnitudes (Fig. 6 *b*).

To estimate actin's relative contribution to sarcomere compliance, the varying stress and strain on the filaments within the overlap zone of the sarcomere must be taken into account. The effect of the distribution of strains can be approximated closely by considering an effective length (L_E) of thin filaments for this purpose as [length of thin filament excluding the Z line] $-$ ⅔ $\times$ [length of an overlap zone] (Eq. A10 of Ford et al., 1981). L_E = [1.12–0.067/2] $-$ ⅔ $\times$ [1.63–0.16]/2 = 0.60 μm at sarcomere length 2.4 μm. The relative contribution of the thin filament to the total compliance in the half-sarcomere is then given by $0.60 \times C_I/c_S$ (Fig. 7). The contribution of the thin filaments was 50–60% in rigor at a sarcomere length of 2.4 μm. The contribution to sarcomere compliance of structures other than thin filaments (cross-bridges, thick filaments, M line, Z line) was 40–50%. The average contributions of thin filaments and remaining elements to total sarcomere compliance at 50–200 kN/m^2 tension were 55 and 45%, respectively.

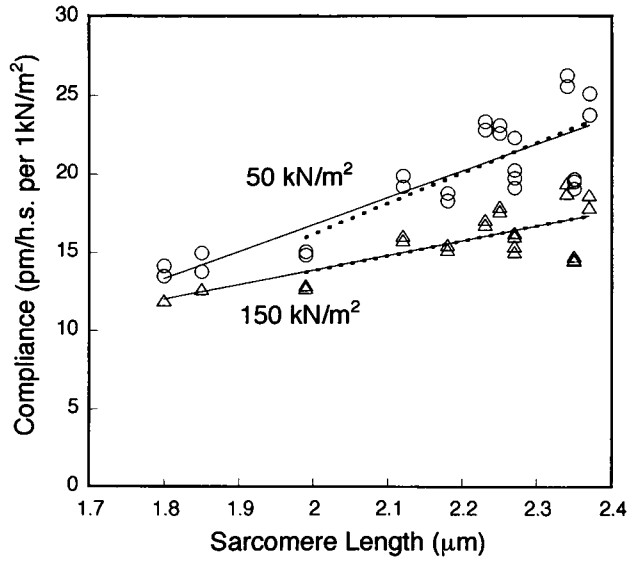

FIGURE 5 Compliance plotted against sarcomere length of the fiber used for Figs. 1, 3, and 4 *a*. Compliance was interpolated to tensions shown, 50 kN/m^2 (○) and 150 kN/m^2 (△), by inserting each tension value into Eq. 3 fitted to the data shown in Fig. 4 *a*. Closely spaced pairs of points are repeated measurements during the same rigor contraction. Using least-squares, compliance data (c_S) at each tension were fitted by the line $c_S = (\frac{1}{2} L - 0.85) \cdot C_I + 0.85 \cdot C_R$ (Eq. 2 in text), where L is the measured sarcomere length and C_I and C_R are estimates of compliance per μm of the I band and the remainder of the sarcomere, respectively. The solid lines were fitted to all of the data, and the dashed lines were fitted to the data at 2.0–2.37 μm.

The open symbols in Fig. 7 represent the contribution of thin filaments and other structures to sarcomere compliance at 150 kN/m^2 tension estimated from data restricted to sarcomere lengths $\geq$2.0 μm. On average the proportion of compliance due to thin filaments was greater, although the SEM values were large due to scatter of data within each experiment (e.g., Fig. 5).

Effects of BDM, Ca^{2+}, and dextran on compliance

BDM was used to maintain sarcomere uniformity by suppressing tension during shortening below slack length. To check whether BDM modifies sarcomere compliance, we measured compliance as shown in Fig. 1, but with BDM

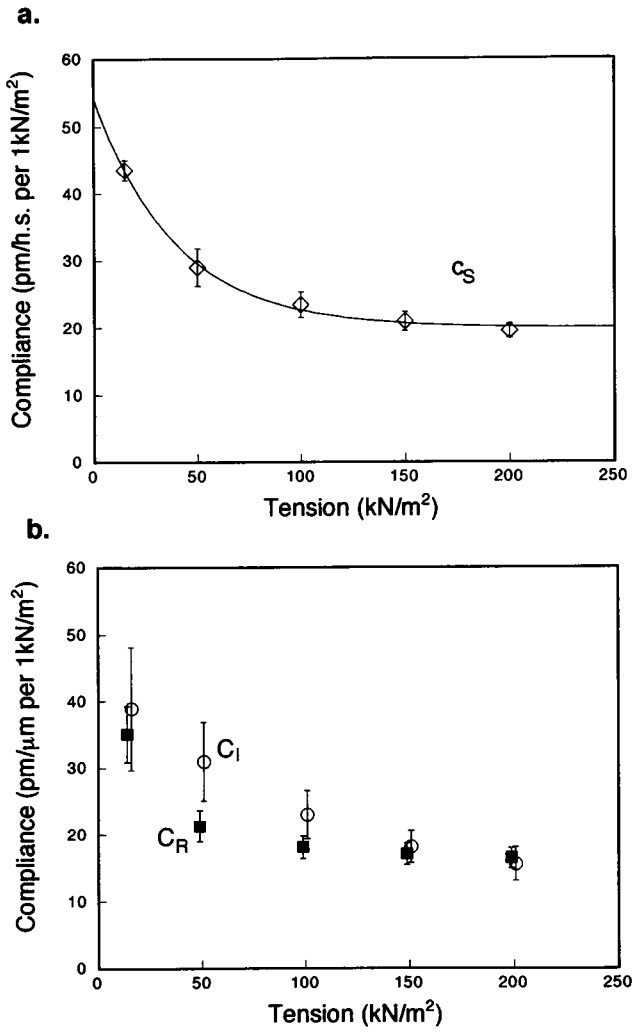

FIGURE 6 Estimated compliance of the sarcomere (c_S, ◇), I bands excluding Z lines (C_I, ○) and structures other than the I bands (C_R, ■) at a sarcomere length of 2.4 μm. Each experiment was analyzed as in Figs. 4 and 5. Data at tension ≥50 kN/m² are means ± SEM, n = 139 data points from six muscle fibers. At 15 kN/m², n = 53 from three fibers. Averages and SEM values were weighted according to the number of data points in each experiment. The curve represents Eq. 3 in the text fitted to the average c_S data; $c_S = 19.9 + 34.9 \cdot \exp(-T/39.3)$ pm stretch per half-sarcomere for each 1 kN/m² force increase. The units for c_S are pm stretch per half-sarcomere for each 1 kN/m² force increase. Units for C_I and C_R are pm stretch per μm filament length for each 1 kN/m² force increase.

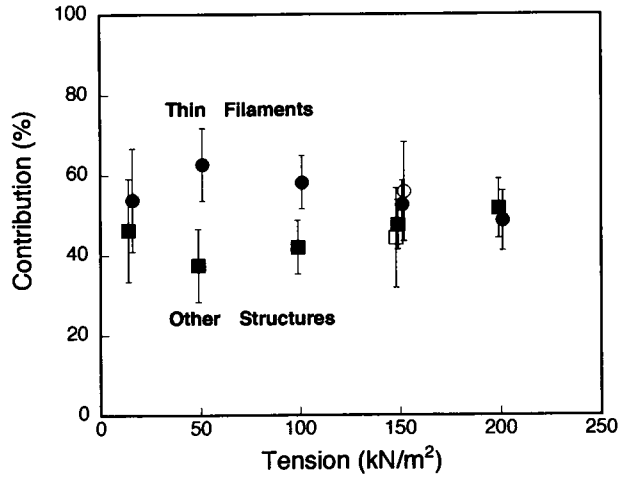

FIGURE 7 Relative contributions to sarcomere compliance. The relative contribution of the thin filaments (●) was calculated as $0.60 \cdot C_I/c_S$ from the data of Fig. 6 at sarcomere lengths 1.8–2.4 μm as explained in the text. The remaining contribution is due to other structures (■). The error bars represent SEM values calculated as in Fig. 6. The open symbols (○, thin filaments; □, other structures) represent data restricted to 2.0- to 2.38-μm sarcomere length.

added during the length pulse sequence. Compliance was also measured without using BDM at all, but in this case compliance could not be measured below slack length. Compliance without BDM was 0.98 ± 0.02 (n = 18) relative to that in the presence of BDM (Fig. 8 *a*), indicating that BDM did not affect adversely the main results.

The lateral spacing between thick filaments changes with the sarcomere length (Rome, 1967), possibly affecting compliance by changing the structure of the cross-bridges or Z line. Lattice spacing was reduced osmotically by adding Dextran T-500 (Pharmacia 17–0320, M_r 500 kDa) to the rigor solution. According to the results of Brenner and Yu (1991), at a sarcomere length of ~2.4 μm, $d_{1,0}$ lattice spacing in rigor is 39 nm in the absence of dextran, 38 nm in the presence of 3% dextran and 36 nm at 6% dextran. Our measurement of rigor compliance was not affected by dextran; compliance values at 3 and 6% dextran were 1.02 ± 0.02% (n = 23) and 1.01 ± 0.02% (n = 24), respectively, of that without dextran respectively (Fig. 8 *b*). These results support the assumption that the compliance of the overlap region is constant in the range of sarcomere lengths used for compliance measurements.

Compliance was measured in most experiments in the absence of Ca^{2+} to avoid activation of proteases (Kasuga and Umazume, 1990). During physiological contractions, however, Ca^{2+} is present in the myoplasm. We measured compliance in the presence of Ca^{2+} using Ca-Rigor solution and normalized to the value in the absence of Ca^{2+}. Compliance in the presence of Ca^{2+} was 1.00 ± 0.02 (n = 20) relative to that in the absence of Ca^{2+} (Fig. 8 *c*), indicating that rigor compliance was not affected by Ca^{2+}. This result was not caused by deterioration of the fibers in the presence of Ca^{2+} because compliance in the absence of Ca^{2+} was the same before and after exposure to Ca^{2+}.

DISCUSSION

Estimation of filament compliance in fibers

Compliance, the reciprocal of stiffness, is a convenient parameter because the total compliance of a series mechanical structure like the sarcomere is the sum of the compliances of its various components. These include the thick filament bare zone, the filament overlap zone, the nonoverlap region of the thin filaments (I band), and the Z line. If all of these components are constant as sarcomere length is

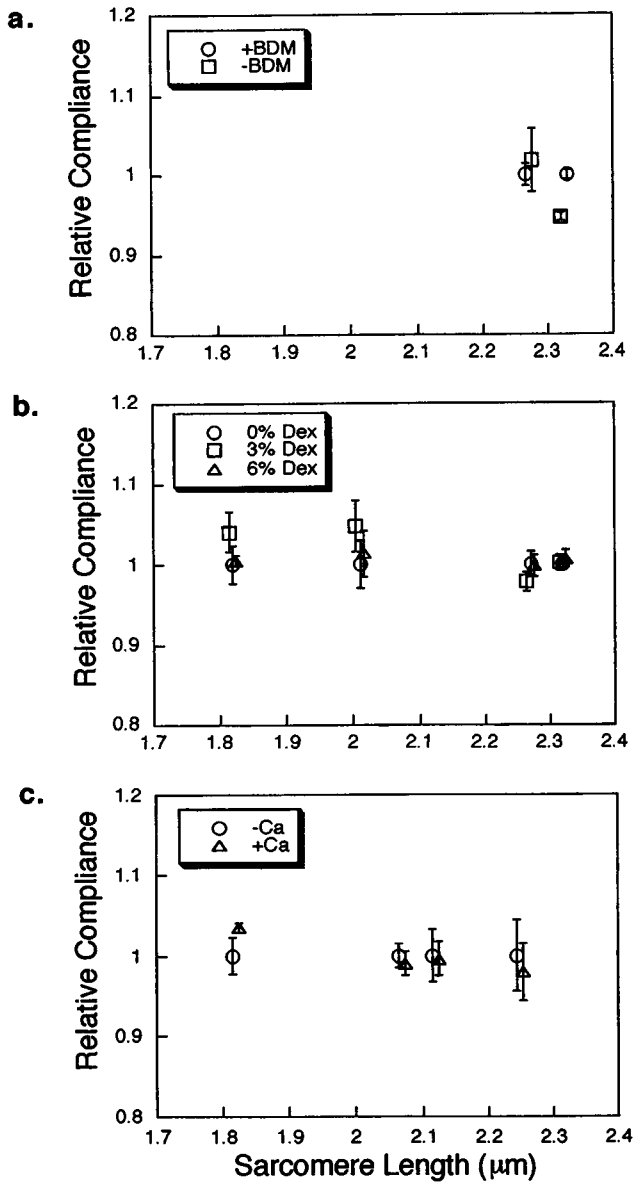

FIGURE 8 Effects of BDM (*a*), Dextran T-500 (*b*), and Ca^{2+} (*c*) on the rigor sarcomere compliance. Compliance in each case was determined relative to that in standard conditions without BDM, dextran or Ca^{2+} in the bathing medium. The error bars are ±SEM, n = 4–13, 6.9 on average. (*a*) Compliance in the presence (○) and the absence (□) of BDM. (*b*) Compliance at 0% (○), 3% (□), and 6% (△) Dextran T-500. (*c*) Compliance in the absence (○) and the presence (△) of 30 μM free Ca^{2+}.

varied except for the I band thin filaments, then changes in sarcomere compliance (Fig. 5) can be attributed to variation of the I band length (Fig. 2). The 40–60% contribution of thin filaments to sarcomere compliance estimated this way is two- to threefold higher than previous values obtained from mechanical studies (Ford et al., 1981; Julian and Morgan, 1981; Bagni et al., 1990). There are several factors that enhance the reliability of the present data relative to those earlier studies.

The present measurements were conducted with rabbit fibers that have longer thin filaments than amphibian muscle, extending the range of sarcomere lengths with complete overlap of the cross-bridge region of the thick filaments. The compliance was measured in rigor, which confers several advantages over compliance measurements on active fibers. The affinity of myosin for actin in the absence of nucleotide is very high (Margossian and Lowy, 1973), and virtually all myosin heads in the overlap zone are thought to attach to actin in rigor (Cooke and Franks, 1980; Thomas and Cooke, 1980; Lovell et al., 1981). Thus, variation in the proportion of cross-bridges attached is of less concern than in actively contracting fibers. Another advantage is that the quick tension recovery observed in actively contracting fibers after a length change (A. F. Huxley and Simmons, 1971) is virtually absent in rigor (Kawai and Brandt, 1980; Fig. 3 here). Length change and tension change could be measured easily within the time resolution of our mechanical transducers. We obtained sarcomere length change signals from a central region of the fiber away from the end attachment points and enhanced the resolution and signal-to-noise ratio by averaging repeated length steps (Fig. 3 *c–f*). The 30–70% variation of fiber compliance with sarcomere length used to estimate the filament compliance was statistically significant (e.g., Fig. 5), and the data from every fiber were consistent with substantial compliance in the thin filaments (Fig. 7).

A possible problem at the shortest lengths used in the present work is that double-overlap between the thin filaments (Fig. 2 *b*) might interfere with cross-bridge attachment and thereby *increase* compliance at short lengths. When we restricted the analysis to striation spacings ≥2.0 μm, the estimated contribution from thin filaments was slightly higher (Figs. 5 and 7), suggesting that cross-bridge attachment is incomplete in the zone of double-overlapped thin filaments. The 40–70% contribution by the thin filaments (including uncertainties), estimated from data at 1.8–2.4 μm, thus, is a lower limit. If the thick filaments in the H zone or M line are compliant, the cross-linking by double-overlapped thin filaments possibly could *decrease* the compliance. The results comparing estimated filament contribution from data at ≥2.0 μm with that from 1.8–2.4 μm (Figs. 5 and 7) make that possibility unlikely. The double-overlap region might also reduce compliance because of interference with filament sliding, but the finding (Fig. 1) that in the presence of Ca^{2+}, ATP, and BDM, fibers would shorten to 1.8 μm or less without developing appreciable force implies that filaments slide freely into the double-overlap range.

BDM was used to obtain short, uniform sarcomere lengths. BDM did not otherwise modify rigor compliance (Fig. 8 *a*), suggesting that BDM does not affect the rigor actomyosin complex (Horiuti et al., 1988). The BDM technique was successful as judged by the small variability of sarcomere length (SD only 0.03 μm) directly observed with a compound microscope. The effect of the small residual sarcomere nonuniformity can be assessed by considering the fiber compliance as the sum of individual sarcomere compliances. Full overlap of the cross-bridge region of the thick filaments occurs at sarcomere lengths of 2.4 μm

and below (Fig. 2 *a*). At average sarcomere lengths below 2.4 − 0.03 = 2.37 μm, where most of the data were obtained, virtually all of the sarcomeres were at full overlap. From Eq. 2, fiber compliance (c_F) for the n half-sarcomeres in the fiber is given by

$$c_F = \sum_{i=1}^{n} [(L_i - L_R) \cdot C_I + L_R \cdot C_R] = n \cdot [(\langle L_i \rangle - L_R) \cdot C_I + L_R \cdot C_R], \quad (4)$$

where the L_i values represent individual sarcomere lengths and $\langle L_i \rangle$ is the mean sarcomere length. This result is equivalent to Eq. 2 showing that at lengths below ~2.37 μm, variation between individual sarcomeres does not bias the total fiber compliance.

The simple relationship between sarcomere length and compliance (Eqs. 2 and 4) is based on several further assumptions. Z lines and thick filament bare zones would not be expected to change compliance with sarcomere length. If lateral spacing between the filaments varies with sarcomere length, then the compliance of the cross-bridges, either subfragment-1 or subfragment-2, might change (Rome, 1967; Matsubara et al., 1984). However, 3 or 6% dextran added to the medium did not change fiber compliance in rigor (Fig. 8 *b*). The compliance of the cross-bridges, therefore, would not change appreciably with changes in sarcomere length in the present conditions.

Elasticity of parallel components, mainly residual elements of the sarcolemma and connectitin (connectin, titin; Higuchi and Umazume, 1986), can be estimated in relaxing solution when myosin is detached from the thin filaments. Compliance of skinned fibers at L = 2.2–2.4 μm in relaxing solution is greater than 10-nm elongation per half-sarcomere for 1 kN/m^2 of force, a value large enough to be ignored relative to rigor compliance. Slack length of the fibers was ~2.2 μm. If compliances of the parallel elements were lower at $L < 2.2$ μm, a resistive force would prevent the fibers from shortening at the low active tension developed in the Act-BDM solution. The observed shortening indicates that parallel elasticity can also be neglected at $L < 2.2$ μm.

The lengths of thin and thick filaments and the bare zone are necessary parameters for estimating the filament compliance. Recently Sosa et al. (1994) measured filament lengths in rabbit skinned fibers very precisely. They found that the lengths of thin and thick filaments are constant in relaxation, rigor, and contraction for sarcomere lengths between ~1.7 and ~3.4 μm. The length of the thick filament bare zone has also been determined accurately (Craig, 1977).

Thin filaments are composed mainly of actin, tropomyosin, troponin, and nebulin. Tropomyosin and nebulin bind to actin filaments along most of their length, and troponin binds to tropomyosin at 38-nm intervals (Ohtsuki, 1974; Wangand Wright, 1988). The mechanical compliance thus may vary with a 38-nm periodicity, but at the 100-nm scale relevant to the present experiments the filaments can be considered uniform. Thus compliance from the thin filaments is proportional to the length of the non-overlap region and the remaining compliances in the sarcomere are virtually constant in the present conditions.

Compliance of the thin filament

Thin filament compliance (C_I) per μm of length, determined by fitting Eq. 2 to sarcomere compliance as in Fig. 5, gave compliance values shown in Fig. 6. Both thin filament (C_I) and sarcomere (c_S) compliance were greater at low tension than at high tension. The change of C_I with force may indicate either that the elasticity of the thin filaments is nonlinear or that some of the filaments are slack at low tension.

Very high resolution x-ray diffraction experiments have recently revealed evidence for extension of thin filaments during development of force in intact frog muscles (H. E. Huxley et al., 1994; Wakabayashi et al., 1994). The 2.7-nm meridional x-ray reflection, which arises from the axial repeat of the actin monomers, shifts by 0.2–0.3%, due to the active force applied to the filaments. The present results are consistent with the degree of extensibility shown by the x-ray experiments.

The sarcomere compliance due to thin filaments can be related to individual filament compliance by considering the number of thin filaments in a cross-sectional area. The thin filament compliance we measured corresponds to 15.6–23.0 pm stretch per μm of filament length per 1 kN/m^2 force increase in the 100–200 kN/m^2 force range. Taking the $d_{1,0}$ lattice spacing as 39 nm (Brenner and Yu, 1991), and the fraction of fiber cross section occupied by myofibrils as 0.83 (Mobley and Eisenberg, 1975), there are 0.95×10^{15} thin filaments per m^2 of fiber cross section. The compliance measured here then corresponds to 14.8–21.9 pm/pN for an individual 1-μm-long filament. This range includes the value 15 pm/pN (stiffness = 65 pN/1 nm stretch of a 1-μm-long filament), obtained by direct measurements on individual actin-tropomyosin filaments in vitro (Kojima et al., 1994).

Force-extension curves of sarcomere components

Using the present data on sarcomere and thin filament elasticity, we can calculate approximate force-extension curves for various components of the sarcomere at L = 2.4 μm. In Fig. 6, the relationship between sarcomere compliance (c_S) per half-sarcomere and tension (T) in rigor is shown to be given by the curve $c_S = 19.9 + 34.9 \cdot \exp(-T/39.3)$ pm/h.s. per 1 kN/m^2 stretch (Eq. 3). We use this curve down to zero tension to calculate the sarcomere force-extension curve because the lowest average tension in Fig. 6, 15 kN/m^2, includes data from tension steps spanning 10–40 kN/m^2. The overall extension of the sarcomere, ΔL_S,

by stretch is calculated by integrating the compliance (c_S) with each increment of applied tension (dT):

$$\Delta L_S = \int_0^{T_0} c_S \, dT, \quad (5)$$

where ΔL_S is the extension in pm and T_0 is the tension applied to the fiber in kN/m^2. Substituting the above relation for c_S, we obtain

$$\Delta L_S = 19.9 \cdot T_0 + 1372 \cdot [1 - \exp(-T_0/39.3)]. \quad (6)$$

According to this expression, a force of 150 kN/m^2, comparable with the active force at 10°C, stretches the half-sarcomere by 4.3 nm in rigor. The rigor force-extension curve (Eq. 5) is plotted in Fig. 9 *a* (curve ΔL_S). For comparison with the situation in an active fiber, extension is plotted relative to the length at 150 kN/m^2 force. From the data in Fig. 7, extension due to the thin filaments (curve ΔL_A in Fig. 9 *a*) is taken as 55% of 4.3 nm or 2.4 nm. Residual extension (curve ΔL_{MZ}), intercepting the abscissa at 1.9 nm, is due to the extension of backbone of thick filament, myosin S-1, S-2, and the Z line. The force-extension relations are nonlinear because sarcomere and thin filament compliance are increased at low tension.

Fibers are ~1.25-fold more compliant in active contraction (with Ca^{2+} and ATP present) than in rigor (Goldman and Simmons, 1977; Higuchi and Goldman, 1991), implying an extension of the sarcomere compliance by 5.4 nm (=1.25 × 4.3 nm) during contraction at tension of 150 kN/m^2. The increased compliance is caused probably either by reduction of the number of attached cross-bridges or by increased compliance in individual cross-bridges. The intensities of equatorial x-ray reflections suggest that fewer myosin heads are bound to the thin filaments in actively contracting muscle than in rigor (Matsubara et al., 1975; Haselgrove and H. E. Huxley, 1973), but changes in the shape of myosin with nucleotide binding are also possible (Wakabayashi et al., 1992). In either case, at a force of 150 kN/m^2, the contribution of the thin filaments to mechanical extension of the sarcomere would be the same as in rigor, 2.4 nm, and the remaining components would be under 3.0-nm strain. The relative contribution of thin filaments, therefore, is 2.4/5.4 = 44%. This value is larger than reported values (less than ~20%, Ford et al., 1981; 19%, Bagni et al., 1990) but consistent with the recent x-ray diffraction experiments discussed earlier (H. E. Huxley et al., 1994; Wakabayashi et al., 1994). Simulated force-extension curves during isometric contraction are plotted in Fig. 9 *b* assuming the sarcomere to be 1.25 times as compliant as in rigor. The increase in compliance is attributed to changes of either the number or compliance of the myosin heads.

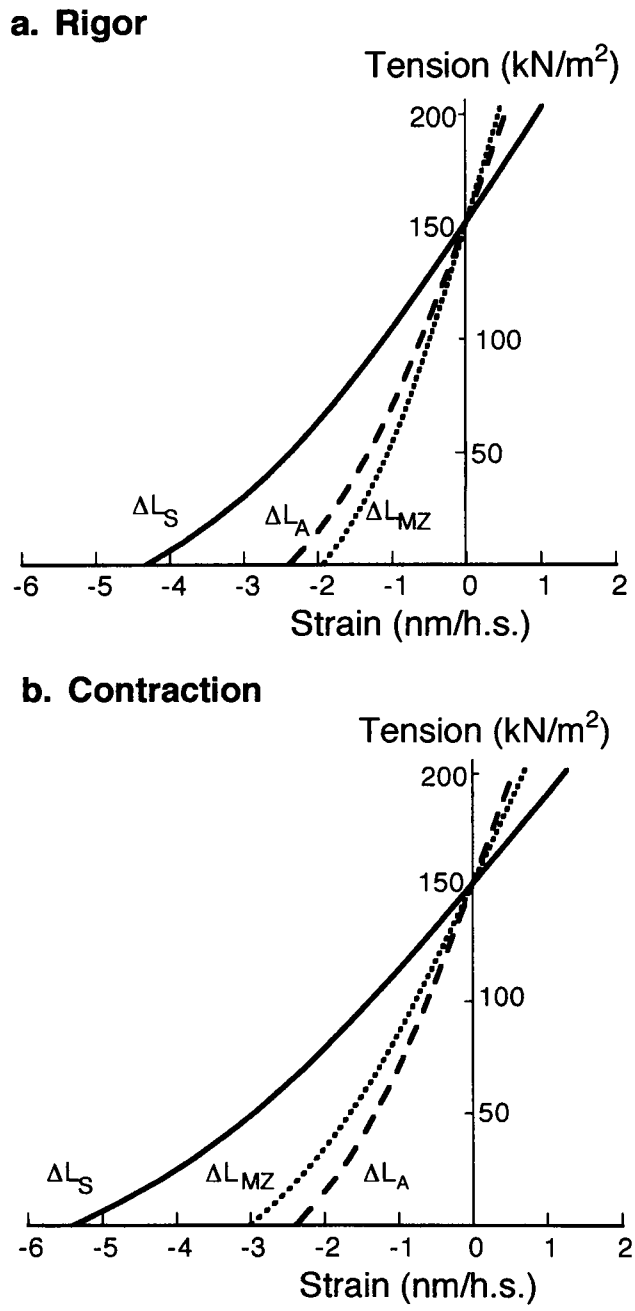

FIGURE 9 Force-extension curves of sarcomere components. Extension was calculated per half-sarcomere at a sarcomere length of 2.4 μm. (*a*) Force-extension curves in rigor. The sarcomere extension (ΔL_S) was calculated by integrating the compliance (c_S in Fig. 6) with each increment of applied tension. The abscissa is plotted relative to the length at 150 kN/m^2. The extensions of thin filaments (ΔL_A) and other structures (ΔL_{MZ}) were calculated as 0.55 and 0.45, of ΔL_S, respectively. (*b*) Force-extension curves in contraction. The sarcomere extension in contraction (ΔL_S) is assumed to be 1.25-fold higher than that in rigor. Extension of the thin filaments in contraction (ΔL_A) is assumed to be the same as in rigor. The extension of the other structures (ΔL_{MZ}) is the difference between ΔL_S and ΔL_A.

Compliance of myosin heads

If the thick filaments, myosin subfragment-2 (S-2), and the Z line are all much stiffer than the myosin heads (S-1) and actin, the 3.0-nm extension in structures other than thin filaments during contraction would be attributed to S-1. Recently, x-ray diffraction experiments, however, revealed that the backbone of the thick filament elongates when a

muscle is stretched during isometric contraction (H. E. Huxley et al., 1994; Wakabayashi et al., 1994). Estimating the amount of compliance in the thick filaments due to mechanical load from the x-ray data is complicated by changes in the myosin-based periodicities due to activation or cross-bridge attachment, but Wakabayashi and co-workers estimated the contribution of thick filaments to sarcomere compliance at ~0.6 that of the thin filaments. If that estimate of the relative contributions of the two sets of filaments is correct, then thick filaments would contribute 1.4 nm out of the total 5.4-nm strain during contraction. Assuming no other significant contributions, the cross-bridge (S-1) compliance would be extended by 5.4 − 2.4 − 1.4 = 1.6 nm. If the Z line and subfragment-2 are compliant, the extension of S-1 is still smaller. Several experiments suggest that the elastic part of the cross-bridge is between the nucleotide-binding and the light chain-binding regions of the S-1 head (Yanagida, 1985; Rayment et al., 1993; Berger et al., 1994; Allen et al., 1995).

Filament compliance alters the interpretation of many mechanical experiments that were based on the assumption that rigid filaments would faithfully transmit applied length changes to the cross-bridges. Fiber stiffness (the reciprocal of compliance) has been used to estimate the relative number of cross-bridges attached under various physiological conditions. The effect of filament compliance on this estimate is to decrease the number of attachments implicated by a given stiffness relative to rigor. For instance, the well known temporal lead of stiffness before force during the onset of a tetanus (Cecchi et al., 1982; Ford et al., 1986; Bagni et al., 1988) might be explained by filament compliance. Effects on tension recovery after quick length changes and the energetics of the force generating step were reviewed briefly by Goldman and A. F. Huxley (1994).

We thank Professor Sir Andrew F. Huxley and Dr. Martin Pring for helpful comments.

This work was supported by National Institutes of Health grant AR42333 and the Muscular Dystrophy Associations of America.

REFERENCES

Allen, T. St. C., C. Sabido-David, N. Ling, M. Irving, and Y. E. Goldman. 1995. Transients of fluorescence polarization following quick length changes or photolysis of caged ATP in skeletal muscle fibers labeled with rhodamine on the regulatory light chain. *Biophys. J.* 68:81s–86s.

Bagni, M. A., G. Cecchi, and M. Schoenberg. 1988. A model of force production that explains the lag between cross-bridge attachment and force after electrical stimulation of striated muscle fibers. *Biophys. J.* 54:1105–1114.

Bagni, M. A., G. Cecchi, F. Colomo, and C. Poggesi. 1990. Tension and stiffness of frog muscle fibres at full filament overlap. *J. Muscle Res. Cell Motil.* 11:371–377.

Berger, C. L., S. Karki, and Y. E. Goldman. 1994. Fluorescence polarization of acetamidotetramethylrhodamine (ATR) covalently bound to SH-1 in rabbit *psoas* muscle fibers following rapid length changes. *Biophys. J.* 66:189*a*. (Abstr.)

Brenner, B., and L. C. Yu. 1991. Characterization of radial force and radial stiffness in Ca^{2+}-activated skinned fibres of the rabbit psoas muscle. *J. Physiol.* 441:703–718.

Cecchi, G., P. J. Griffiths, and S. Taylor. 1982. Muscular contraction: kinetics of crossbridge attachment studied by high-frequency stiffness measurements. *Science.* 217:70–72.

Cooke, R., and K. Franks. 1980. All myosin heads form bonds with actin in rigor rabbit skeletal muscle. *Biochemistry.* 19:2265–2269.

Craig, R. 1977. Structure of A-segments from frog and rabbit skeletal muscle. *J. Mol. Biol.* 109:69–81.

Ford, L. E., A. F. Huxley, and R. M. Simmons. 1977. Tension responses to sudden length change in stimulated frog muscle fibres near slack length. *J. Physiol.* 269:441–515.

Ford, L. E., A. F. Huxley, and R. M. Simmons. 1981. The relation between stiffness and filament overlap in stimulated frog muscle fibres. *J. Physiol.* 311:219–249.

Ford, L. E., A. F. Huxley, and R. M. Simmons. 1986. Tension transients during the rise of tetanic tension in frog muscle fibres. *J. Physiol.* 372:595–609.

Fujime, S. 1970. Quasi-elastic light scattering from solutions of macromolecules. II. Doppler broadening of light scattered from solutions of semi-flexible polymers, F-actin. *J. Phys. Soc. Japan.* 29:751–759.

Goldman, Y. E., M. G. Hibberd, and D. R. Trentham. 1984. Relaxation of rabbit psoas muscle fibres from rigor by photochemical generation of adenosine-5′-triphosphate. *J. Physiol.* 354:577–604.

Goldman, Y. E. 1987. Measurement of sarcomere shortening in skinned fibers from frog muscle by white light diffraction. *Biophys. J.* 52:57–68.

Goldman, Y. E., and R. M. Simmons. 1977. Active and rigor muscle stiffness. *J. Physiol.* 269:55P–57P.

Goldman, Y. E., and R. M. Simmons. 1984. Control of sarcomere length in skinned muscle fibres of *Rana temporaria* during mechanical transients. *J. Physiol.* 350:497–518.

Goldman, Y. E., and A. F. Huxley. 1994. Actin compliance: are you pulling my chain? *Biophys. J.* 67:2131–2133.

Hanson, J., and H. E. Huxley. 1955. The structural basis of contraction in striated muscle. *Symp. Soc. Exp. Biol.* 9:228–264.

Haselgrove, J. C., and H. E. Huxley. 1973. X-ray evidence for radial cross-bridge movement and for the sliding filament model in actively contracting skeletal muscle. *J. Mol. Biol.* 77:549–568.

Higuchi, H., and Y. E. Goldman. 1991. Sliding distance between actin and myosin filaments per ATP molecule hydrolysed in skinned muscle fibres. *Nature.* 352:352–354.

Higuchi, H., and S. Takemori. 1989. Butanedione monoxime suppresses contraction and ATPase activity of rabbit skeletal muscle. *J. Biochem.* 105:638–643.

Higuchi, H., and Y. Umazume. 1986. Lattice shrinkage with increasing resting tension in stretched, single skinned fibers of frog muscle. *Biophys. J.* 50:385–389.

Higuchi, H., T. Yanagida, and Y. E. Goldman. 1994. Compliance of thin filaments in skinned fibers of rabbit psoas muscle. *Biophysics (Japan).* 34:S29.

Horiuti, K., H. Higuchi, Y. Umazume, M. Konishi, O. Okazaki, and S. Kurihara. 1988. Mechanism of action of 2,3-butanedione 2-monoxime on contraction of frog skeletal muscle fibres. *J. Muscle Res. Cell Motil.* 9:156–164.

Huxley, A. F. 1957. Muscle structure and theories of contraction. *Prog. Biophys. Biophys. Chem.* 7:255–318.

Huxley, A. F., and R. Niedergerke. 1954. Structural changes in muscle during contraction: interference microscopy of living muscle fibres. *Nature.* 173:971–973.

Huxley, A. F., and R. M. Simmons. 1971. Proposed mechanism of force generation in striated muscle. *Nature.* 233:533–538.

Huxley, H. E., and J. Hanson. 1954. Changes in the cross-striations of muscle during contraction and stretch and their structural interpretation. *Nature.* 173:973–976.

Huxley, H. E., A. Stewart, H. Sosa, and T. Irving. 1994. X-ray diffraction measurements of the extensibility of actin and myosin filaments in contracting muscle. *Biophys. J.* 67:2411–2421.

Julian, F. J., and D. L. Morgan. 1981. Tension, stiffness, unloaded shortening speed and potentiation of frog muscle fibres at sarcomere lengths below optimum. *J. Physiol.* 319:205–217.

Kasuga, N., and Y. Umazume. 1990. Deterioration induced by physiological concentration of calcium ions in skinned muscle fibres. *J. Muscle Res. Cell Motil.* 11:41–47.

Kawai, M., and P. W. Brandt. 1980. Sinusoidal analysis: a high resolution method for correlating biochemical reactions with physiological processes in activated skeletal muscles of rabbit, frog and crayfish. *J. Muscle Res. Cell Motil.* 1:279–303.

Kojima, H., A. Ishijima, and T. Yanagida. 1994. Direct measurement of stiffness of single actin filaments with and without tropomyosin using in vitro nano-manipulation. *Proc. Natl. Acad. Sci. USA.* 91:12962–12966.

Lovell, S. J., P. J. Knight, and W. F. Harrington. 1981. Fraction of myosin heads bound to thin filaments in rigor fibrils from insect flight and vertebrate muscles. *Nature.* 293:664–666.

Margossian, S. S., and S. Lowey. 1973. Substructure of the myosin molecule. IV. Interactions of myosin and its subfragments with adenosine triphosphate and F-actin. *J. Mol. Biol.* 74:313–330.

Matsubara, I., Y. E. Goldman, and R. M. Simmons. 1984. Changes in the lateral filament spacing of skinned muscle fibres when cross-bridges attach. *J. Mol. Biol.* 173:15–33.

Matsubara, I., N. Yagi, and H. Hashizume. 1975. Use of an x-ray television for diffraction of the frog striated muscle. *Nature.* 255:728–729.

Mobley, B. A., and B. R. Eisenberg. 1975. Sizes of components in frog skeletal muscle measured by methods of stereology. *J. Gen. Physiol.* 66:31–45.

Ohtsuki, I. 1974. Localization of troponin in thin filament and tropomyosin paracrystal. *J. Biochem.* 75:753–765.

Oosawa, F., S. Fujime, S. Ishiwata, and K. Mihashi. 1973. Dynamic property of F-actin and thin filament. *Cold Spring Harbor Symp. Quant. Biol.* 37:277–285.

Rayment, I., W. R. Rypniewski, K. Schmidt-Bäse, R. Smith, D. R. Tomchick, M. M. Benning, D. A. Winkelmann, G. Wesenberg, and H. M. Holden. 1993. Three-dimensional structure of myosin subfragment-1: a molecular motor. *Science.* 261:50–58.

Rome, E. 1967. Light and x-ray diffraction studies of the filament lattice of glycerol-extracted rabbit psoas muscle. *J. Mol. Biol.* 27:591–602.

Schachat, F. H., A. C. Canine, M. M. Briggs, and M. C. Reedy. 1985. The presence of two skeletal muscle α-actinins correlates with troponin-tropomyosin expression and Z-line width. *J. Cell Biol.* 101:1001–1008.

Sosa, H., D. Popp, G. Ouyang, and H. E. Huxley. 1994. Ultrastructure of skeletal muscle fibers studied by a plunge quick freezing method: myofilament lengths. *Biophys. J.* 67:283–292.

Tawada, K., and M. Kimura. 1984. Stiffness of glycerinated rabbit *psoas* fibers in the rigor state. *Biophys. J.* 45:593–602.

Thomas, D. D., and R. Cooke. 1980. Orientation of spin-labeled myosin heads in glycerinated muscle fibers. *Biophys. J.* 32:891–906.

Wakabayasi, K., Y. Sugimoto, H. Tanaka, Y. Ueno, Y. Takezawa, and Y. Amemiya. 1994. X-ray diffraction evidence for the extensibility of actin and myosin filaments during muscle contraction. *Biophys. J.* 67: 2422–2435.

Wakabayashi, K., M. Tokunaga., I. Kohno, Y. Sugimoto, T. Hamanaka, Y. Takezawa, T. Wakabayashi, and Y. Amemiya. 1992. Small-angle synchrotron x-ray scattering reveals distinct shape changes of the myosin head during hydrolysis of ATP. *Science.* 258:443–447.

Wang, K., and J. Wright. 1988. Architecture of the sarcomere matrix of skeletal muscle: immunoelectron microscopic evidence that suggests a set of parallel inextensible nebulin filaments anchored at the Z line. *J. Cell Biol.* 107:2199–2212.

Yanagida, T. 1985. Angle of active site of myosin heads in contracting muscle during sudden length changes. *J. Muscle Res. Cell Motil.* 6:43–52.